

# Deforming Composite Grids for Fluid-Structure Interaction: Overcoming the Added-Mass Instability for Compressible Fluids and Elastic Solids

Jeff Banks, Bill Henshaw

Lawrence Livermore National Laboratory

DOE Applied Mathematics Program Meeting  
Washington, DC, October 17, 2011

# Collaborators

Donald Schwendeman

Department of Mathematical Sciences  
Rensselaer Polytechnic Institute

## Support

Department of Energy  
Office of Advanced Scientific Computing Research  
Applied Mathematics Program  
Lawrence Livermore National Laboratory  
National Science Foundation

## We are developing a new interface projection methodology to eliminate added mass instabilities in partitioned schemes

- Traditional partitioned FSI algorithms
  1. advance fluid (using interface velocity/position from the solid)
  2. advance solid (apply fluid forces to the solid)
  - This approach suffers instability for light solids (added mass instability)
  
- We are developing a new interface projection approach
  1. advance fluid
  2. advance solid
  3. project solution at interface
  - This approach can be proven to be stable for all ratios of fluid and solid masses

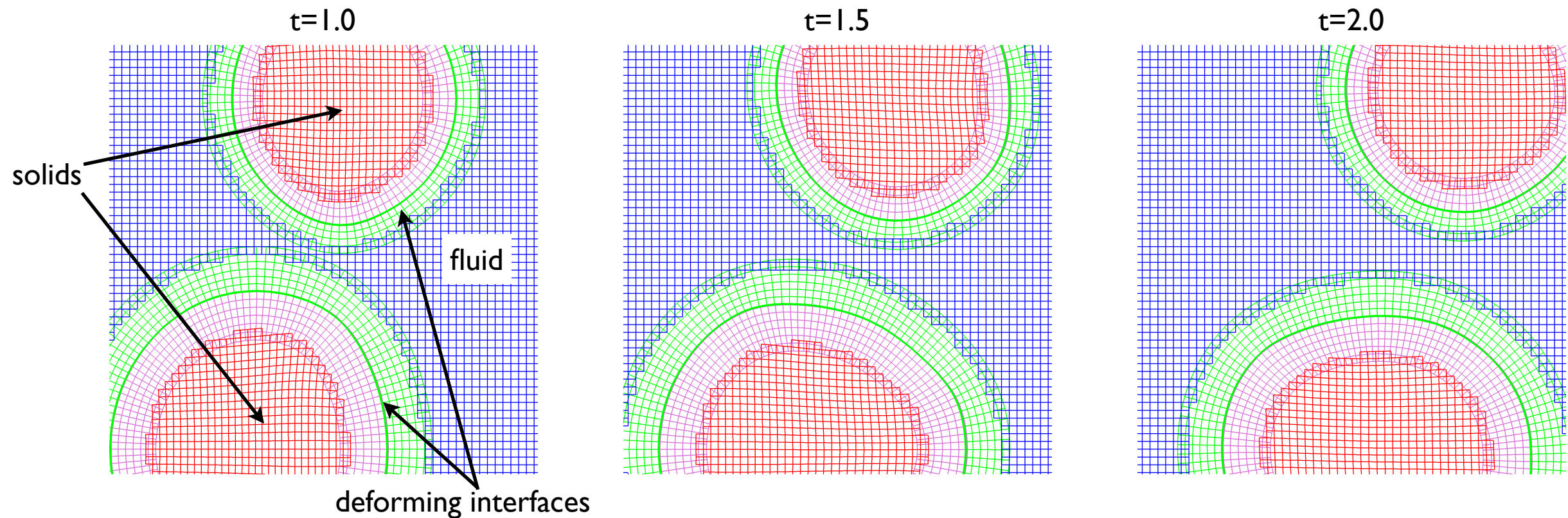
## We are developing a new interface projection methodology to eliminate added mass instabilities in partitioned schemes

- Traditional partitioned FSI algorithms
  1. advance fluid (using interface velocity/position from the solid)
  2. advance solid (apply fluid forces to the solid)
  - This approach suffers instability for light solids (added mass instability)
  
- We are developing a new interface projection approach
  1. advance fluid
  2. advance solid
  3. project solution at interface
  - This approach can be proven to be stable for all ratios of fluid and solid masses



# Deforming Composite Grids (DCGs) are an efficient way to discretize PDEs in deforming and/or moving geometry

- Overlapping grids are the foundation of DCGs



- Benefits of this approach include:
  - Local and rapid grid generation (hyperbolic grid generator)
  - High quality grids even under large displacements and rotations
  - High efficiency through the use of structured and Cartesian grids
  - Grid construction that supports high-order discretizations
- We use the Overture and CG software packages
  - [www.llnl.gov/CASC/Overture](http://www.llnl.gov/CASC/Overture)

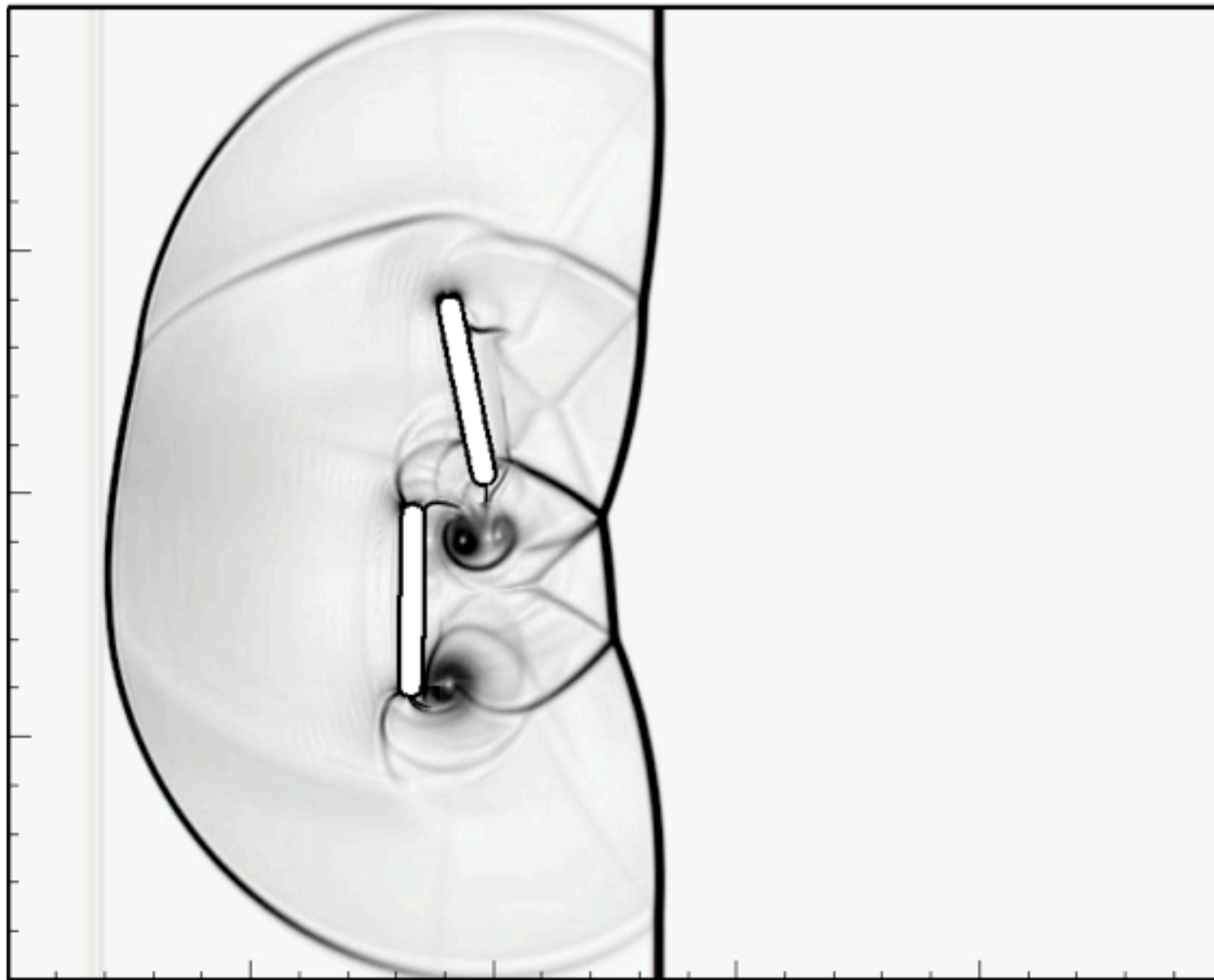
In previous work we have used moving, overlapping grids to couple rigid body motion with high-speed compressible flows

- Example: Mach-2 shock impacting rigid sticks

• WDH, D. W. Schwendeman, *Moving Overlapping Grids with Adaptive Mesh Refinement for High-Speed and Nonreactive Flow*, J. Comput. Phys. **216** (2005)

In previous work we have used moving, overlapping grids to couple rigid body motion with high-speed compressible flows

- Example: Mach-2 shock impacting rigid sticks



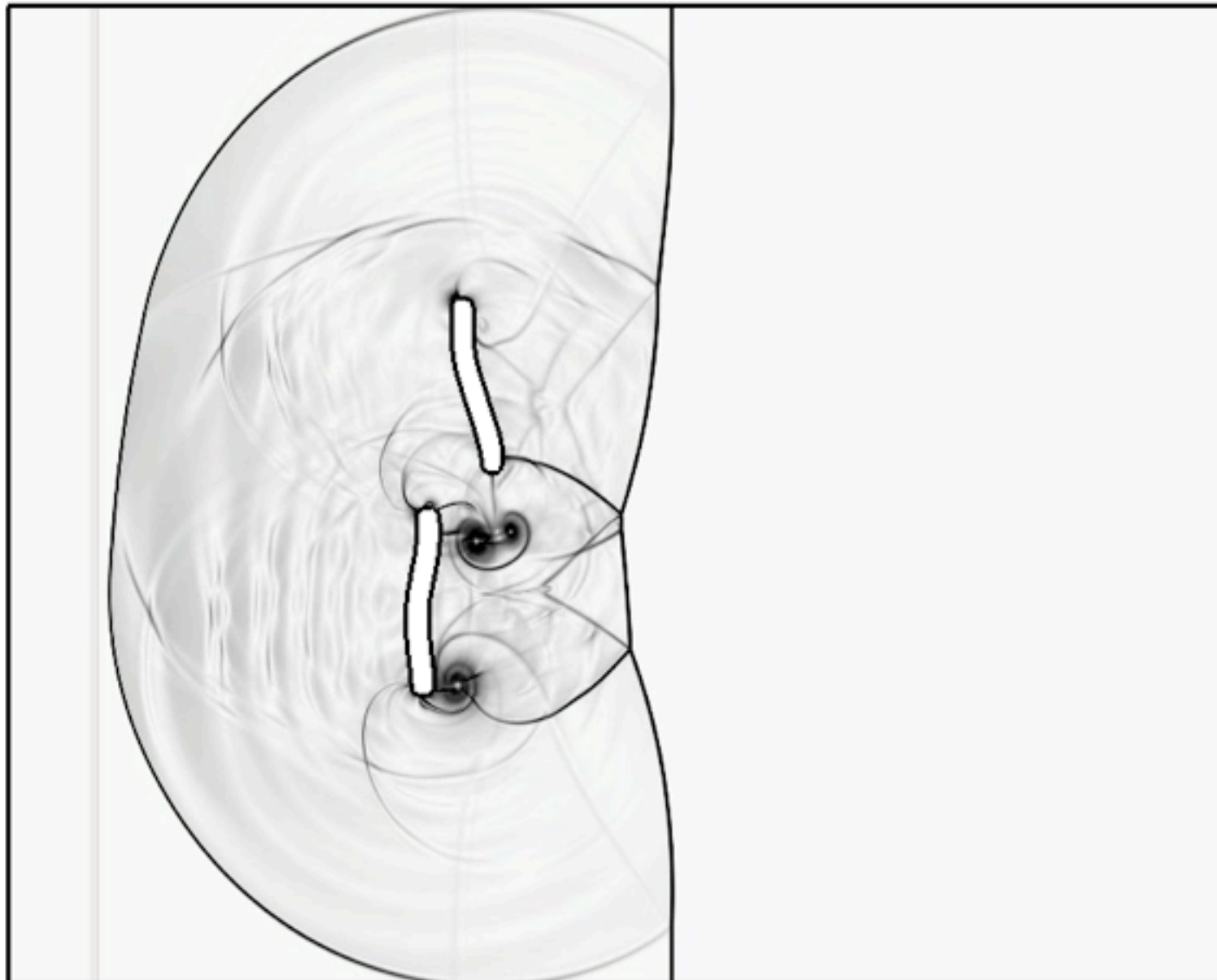
- WDH, D. W. Schwendeman, *Moving Overlapping Grids with Adaptive Mesh Refinement for High-Speed and Nonreactive Flow*, J. Comput. Phys. **216** (2005)

## Goal: perform coupled simulations of compressible fluids and deforming solids

- Mixed Eulerian-Lagrangian approach
  - Fluids: general moving coordinate system with deforming composite grids
  - Solids: fixed reference frame with overlapping grids
  - Boundary fitted deforming grids for fluid-solid interfaces

## Goal: perform coupled simulations of compressible fluids and deforming solids

- Mixed Eulerian-Lagrangian approach
  - Fluids: general moving coordinate system with deforming composite grids
  - Solids: fixed reference frame with overlapping grids
  - Boundary fitted deforming grids for fluid-solid interfaces



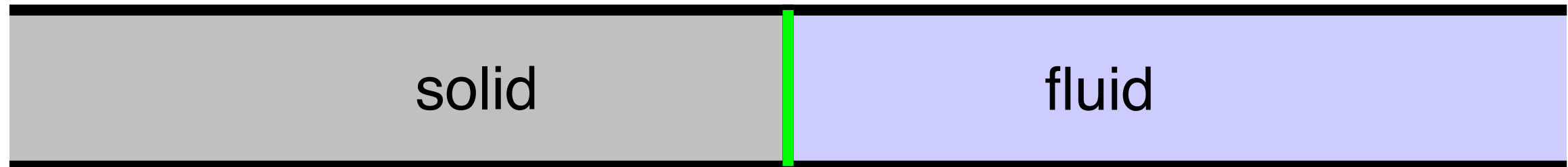
## We pursue a partitioned approach for maximal efficiency and flexibility

- Fluid solver: we solve the inviscid Euler equations with a second-order extension of Godunov's method (cgcns)
  - WDH, D. W. Schwendeman, *Parallel Computation of Three-Dimensional Flows using Overlapping Grids with Adaptive Mesh Refinement*, J. Comput. Phys. **227** (2008)
  - WDH, D. W. Schwendeman, *An Adaptive Numerical Scheme for High-Speed Reactive Flow on Overlapping Grids*, J. Comput. Phys. **191** (2003)
  
- Solid solver: we solve the elastic wave equations as a first-order system with a second-order upwind scheme (cgsm)
  - D. Appelö, JWB, WDH, D. W. Schwendeman, *Numerical Methods for Solid Mechanics on Overlapping Grids: Linear Elasticity*, LLNL-JRNL-422223, submitted
  
- Multidomain coupler: we use an interface projection scheme which is stable across the entire range of material parameters, including for light solids (cgmp)
  - JWB, WDH, D. W. Schwendeman, *Deforming Composite Grids for Solving Fluid Structure Problems*, LLNL-JRNL-493791, submitted
  - JWB, B. Sjögren, *A normal mode stability analysis of numerical interface conditions for fluid-structure interaction*, Commun. Comput. Phys., **10** (2011)

## We pursue a partitioned approach for maximal efficiency and flexibility

- Fluid solver: we solve the inviscid Euler equations with a second-order extension of Godunov's method (cgcns)
  - WDH, D. W. Schwendeman, *Parallel Computation of Three-Dimensional Flows using Overlapping Grids with Adaptive Mesh Refinement*, J. Comput. Phys. **227** (2008)
  - WDH, D. W. Schwendeman, *An Adaptive Numerical Scheme for High-Speed Reactive Flow on Overlapping Grids*, J. Comput. Phys. **191** (2003)
- Solid solver: we solve the elastic wave equations as a first-order system with a second-order upwind scheme (cgsm)
  - D. Appelö, JWB, WDH, D. W. Schwendeman, *Numerical Methods for Solid Mechanics on Overlapping Grids: Linear Elasticity*, LLNL-JRNL-422223, submitted
- **Multidomain coupler: we use an interface projection scheme which is stable across the entire range of material parameters, including for light solids (cgmp)**
  - JWB, WDH, D. W. Schwendeman, *Deforming Composite Grids for Solving Fluid Structure Problems*, LLNL-JRNL-493791, submitted
  - JWB, B. Sjögreen, *A normal mode stability analysis of numerical interface conditions for fluid-structure interaction*, Commun. Comput. Phys., **10** (2011)

We find it useful to investigate a model FSI problem in 1D, the elastic piston problem



Linear Elasticity

$$\begin{cases} \partial_t \bar{u} - \bar{v} = 0 \\ \bar{\rho} \partial_t \bar{v} - \partial_{\bar{x}} \bar{\sigma} = 0 \\ \partial_t \bar{\sigma} - \bar{\rho} c_p^2 \partial_{\bar{x}} \bar{v} = 0 \end{cases}$$

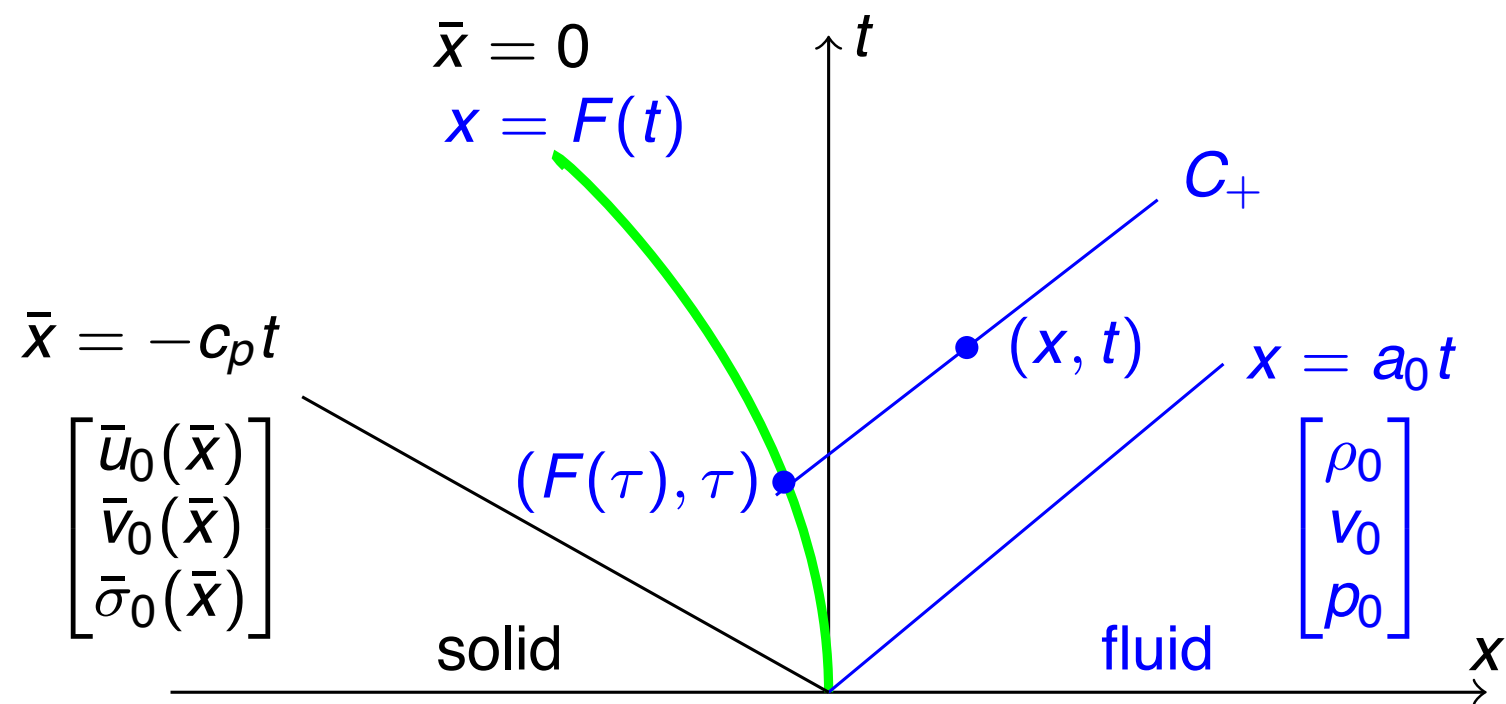
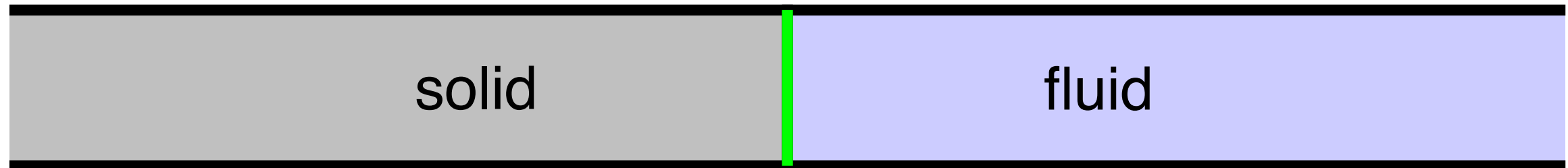
Euler Equations

$$\begin{cases} \partial_t \rho + \partial_x (\rho v) = 0 \\ \partial_t (\rho v) + \partial_x (\rho v^2 + p) = 0 \\ \partial_t (\rho E) + \partial_x (\rho E v + p v) = 0 \end{cases}$$

Interface Coupling Conditions

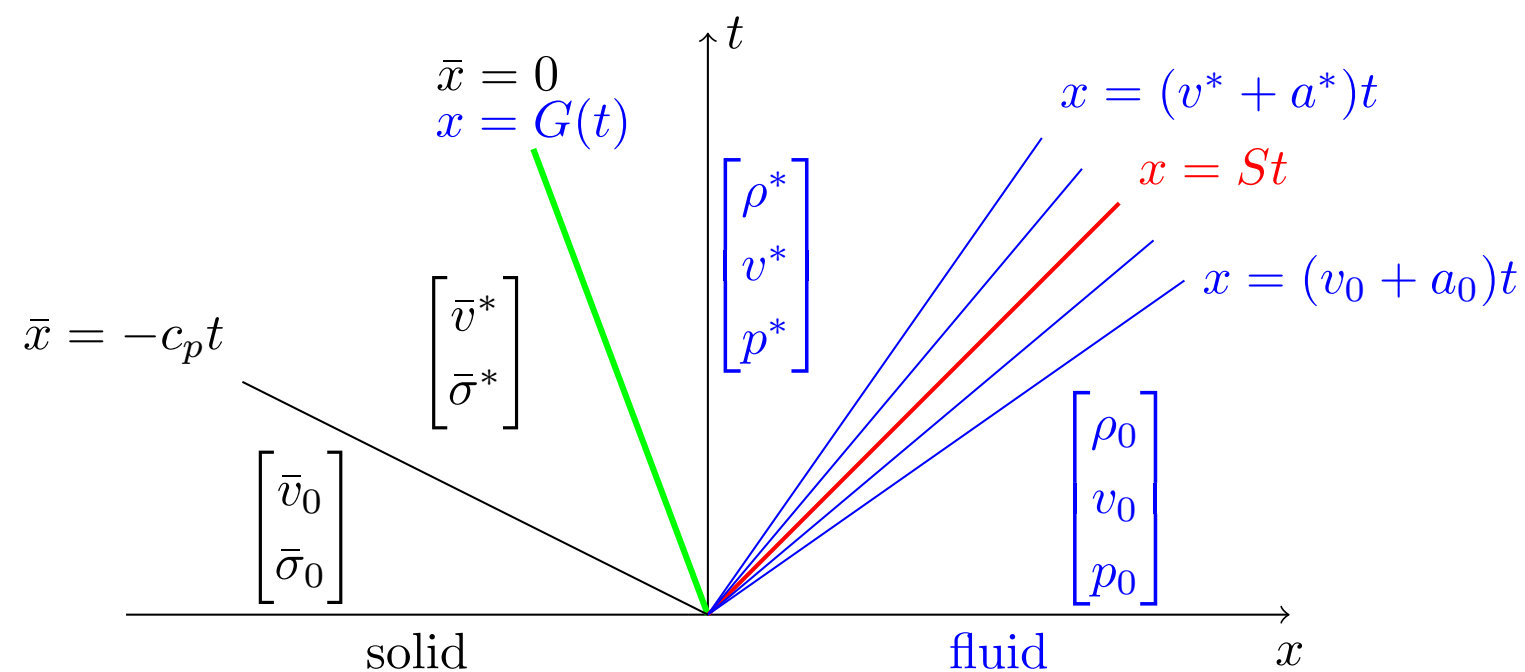
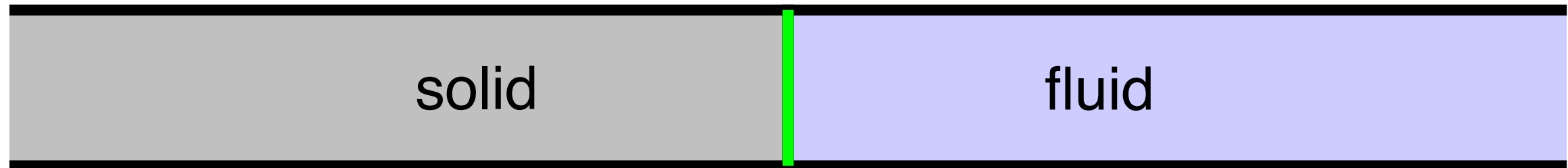
$$\begin{cases} \bar{v}(\bar{x}, t) = v(x, t), \\ \bar{\sigma}(\bar{x}, t) = \sigma(x, t) \equiv -p(x, t) + p_e \end{cases}$$

We find it useful to investigate a model FSI problem in 1D, the elastic piston problem



- For our purposes, exact solutions are obtained in two ways
  - Given initial conditions, solve for  $F(t)$
  - Given  $F(t)$ , solve for initial conditions

## The interface projection scheme can be motivated by investigating the fluid-structure Riemann problem (FSRP)



- This is a specific case of the elastic piston problem
  - Constant states in fluid and solid
- Exact solutions to the linear and nonlinear problem are easily found

## The solution to the linearized (FSRP) can be obtained using characteristics

- The characteristic forms of the linearized equations are

$$\left\{ \begin{array}{l} \text{Solid} \\ d\bar{u}/dt = \bar{v}, \quad \text{on } d\bar{x}/dt = 0, \\ \bar{z}\bar{v} \mp \bar{\sigma} = \bar{z}\bar{v}_0 \mp \bar{\sigma}_0, \quad \text{on } d\bar{x}/dt = \pm c_p, \end{array} \right.$$
$$\left\{ \begin{array}{l} \text{Fluid} \\ a_0^2 \rho + \sigma = a_0^2 \rho_0 + \sigma_0, \quad \text{on } dx/dt = v_0, \\ zv \mp \sigma = zv_0 \mp \sigma_0, \quad \text{on } dx/dt = v_0 \pm a_0, \end{array} \right.$$

- Using the interface conditions gives the solution

$$v^* = \bar{v}^* = \frac{\bar{z}\bar{v}_0 + zv_0}{\bar{z} + z} + \frac{\sigma_0 - \bar{\sigma}_0}{\bar{z} + z}$$

$$\sigma^* = \bar{\sigma}^* = \frac{\bar{z}^{-1}\bar{\sigma}_0 + z^{-1}\sigma_0}{\bar{z}^{-1} + z^{-1}} + \frac{v_0 - \bar{v}_0}{\bar{z}^{-1} + z^{-1}}$$

- Here  $\bar{z} = \bar{\rho}c_p$  and  $z = \rho_0 a_0$  are acoustic impedances

## The solution to the linearized (FSRP) can be obtained using characteristics

- The characteristic forms of the linearized equations are

$$\left\{ \begin{array}{l} \text{Solid} \\ d\bar{u}/dt = \bar{v}, \quad \text{on } d\bar{x}/dt = 0, \\ \bar{z}\bar{v} \mp \bar{\sigma} = \bar{z}\bar{v}_0 \mp \bar{\sigma}_0, \quad \text{on } d\bar{x}/dt = \pm c_p, \end{array} \right.$$
$$\left\{ \begin{array}{l} \text{Fluid} \\ a_0^2 \rho + \sigma = a_0^2 \rho_0 + \sigma_0, \quad \text{on } dx/dt = v_0, \\ zv \mp \sigma = zv_0 \mp \sigma_0, \quad \text{on } dx/dt = v_0 \pm a_0, \end{array} \right.$$

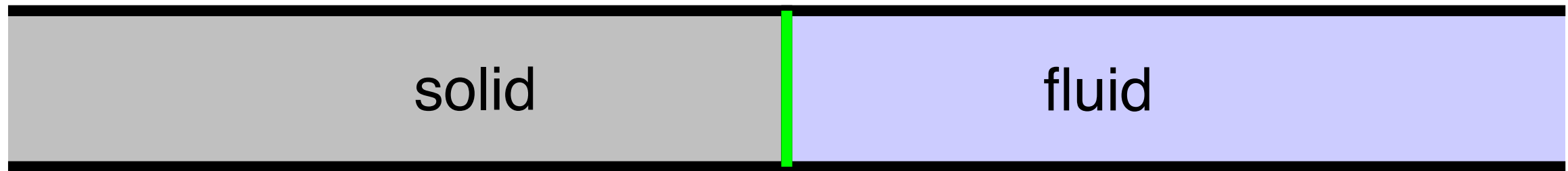
- Using the interface conditions gives the solution

$$v^* = \bar{v}^* = \frac{\bar{z}\bar{v}_0 + zv_0}{\bar{z} + z} + \frac{\sigma_0 - \bar{\sigma}_0}{\bar{z} + z}$$

$$\sigma^* = \bar{\sigma}^* = \frac{\bar{z}^{-1}\bar{\sigma}_0 + z^{-1}\sigma_0}{\bar{z}^{-1} + z^{-1}} + \frac{v_0 - \bar{v}_0}{\bar{z}^{-1} + z^{-1}}$$

- Here  $\bar{z} = \bar{\rho}c_p$  and  $z = \rho_0 a_0$  are acoustic impedances

# The time stepping procedure for the FSI-DCG scheme



The FSI-DCG time stepping algorithm			
Stage	Condition	Type	Assigns
Interior(a)	Predict grid and grid velocity	extrapolation	$G^p, \dot{G}^p$
Interior(b)	Advance $\mathbf{w}_i^n, \bar{\mathbf{w}}_i^n, i = 0, 1, 2, \dots$	PDE	interior, interface
Interface(a)	Compute $[v_I, \sigma_I, \rho_I]$ from FSRP	projection	$v_I, \sigma_I, \rho_I$
Interface(b)	Set $\rho_0^n = \rho_I, p_0^n = p_I, v_0 = \bar{v}_0^n = v_I, \bar{\sigma}_0^n = \sigma_I$	projection	$\mathbf{w}_0^n, \bar{\mathbf{w}}_0^n$
Interface(c)	Correct $\bar{u}_0^n$ , grid and grid velocity	projection	$\bar{u}_0^n, G^n, \dot{G}^n$
Ghost(a)	$\mathbf{w}_{-1}^n = \mathcal{E}_{+1}^{(3)} \mathbf{w}_0^n, \bar{\mathbf{w}}_{-1}^n = \bar{\mathcal{E}}_{+1}^{(3)} \bar{\mathbf{w}}_0^n,$	extrapolation	$\mathbf{w}_{-1}^n, \bar{\mathbf{w}}_{-1}^n$
Ghost(b)	Compute $\dot{v}_0 = (1/\bar{\rho}) \bar{D}_0 \bar{\sigma}_0^n, \dots$	PDE	$\dot{v}_0, \dot{\sigma}_0, \dot{v}_0, \dot{\sigma}_0$
Ghost(c)	Compute $\dot{v}_I, \dot{\sigma}_I$	projection	$\dot{v}_I, \dot{\sigma}_I$
Ghost(d)	Set $(1/\bar{\rho}) \bar{D}_0 \bar{\sigma}_0^n = \dot{v}_I, \dots$	compatibility	$\bar{\sigma}_{-1}, \bar{v}_{-1}^n, p_{-1}^n, v_{-1}^n$

## The solution at the interface is defined in terms of solutions to the FSRP

- Along the interface, the solution is projected using solutions to local FSRPs

$$v_I = \frac{\bar{z}\bar{v}_0 + zv_0}{\bar{z} + z} + \frac{\sigma_0 - \bar{\sigma}_0}{\bar{z} + z}$$
$$\sigma_I = \frac{\bar{z}^{-1}\bar{\sigma}_0 + z^{-1}\sigma_0}{\bar{z}^{-1} + z^{-1}} + \frac{v_0 - \bar{v}_0}{\bar{z}^{-1} + z^{-1}}$$
$$\rho_I = \rho_0(p_I/p_0)^{1/\gamma}$$

- The traditional FSI coupling is the large impedance (mass) limit  $\bar{z} \gg z$ 
  - velocity from solid  $v_I = \bar{v}_0$
  - stress from fluid  $\sigma_I = \sigma_0 = -p_0 + p_e$
- The traditional scheme is unstable for light solids
- The new scheme is stable for any ratio of masses and impedances
- For proofs see JWB, B. Sjögreen, *A normal mode stability analysis of numerical interface conditions for fluid-structure interaction*, Commun. Comput. Phys., **10** (2011)
- Note: for some difficult problems there are advantages to using the nonlinear FSRP

## The solution at the interface is defined in terms of solutions to the FSRP

- Along the interface, the solution is projected using solutions to local FSRPs

$$v_I = \frac{\bar{z}\bar{v}_0 + zv_0}{\bar{z} + z} + \frac{\sigma_0 - \bar{\sigma}_0}{\bar{z} + z}$$
$$\sigma_I = \frac{\bar{z}^{-1}\bar{\sigma}_0 + z^{-1}\sigma_0}{\bar{z}^{-1} + z^{-1}} + \frac{v_0 - \bar{v}_0}{\bar{z}^{-1} + z^{-1}}$$
$$\rho_I = \rho_0(p_I/p_0)^{1/\gamma}$$

- The traditional FSI coupling is the large impedance (mass) limit  $\bar{z} \gg z$ 
  - velocity from solid  $v_I = \bar{v}_0$
  - stress from fluid  $\sigma_I = \sigma_0 = -p_0 + p_e$
- The traditional scheme is unstable for light solids
- The new scheme is stable for any ratio of masses and impedances
- For proofs see JWB, B. Sjögreen, *A normal mode stability analysis of numerical interface conditions for fluid-structure interaction*, Commun. Comput. Phys., **10** (2011)
- Note: for some difficult problems there are advantages to using the nonlinear FSRP

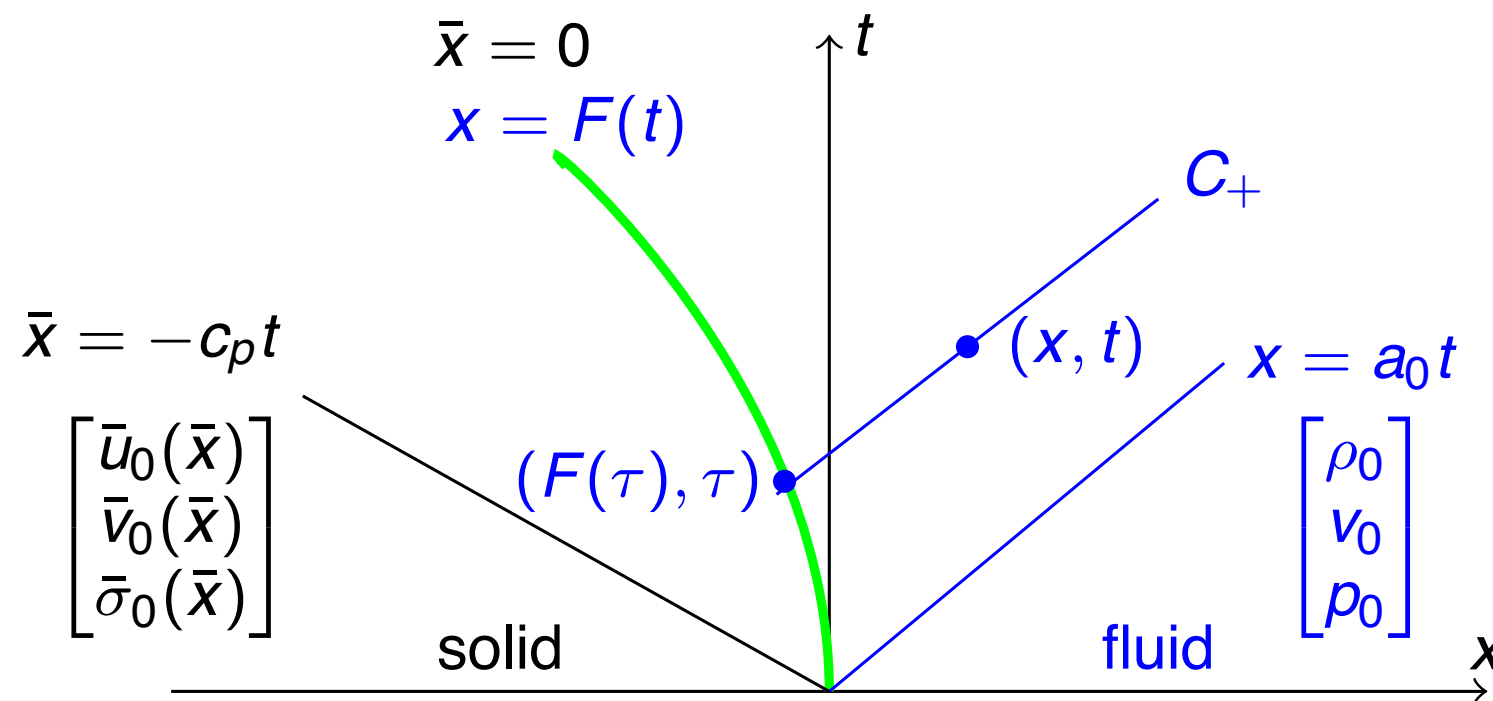
## The solution at the interface is defined in terms of solutions to the FSRP

- Along the interface, the solution is projected using solutions to local FSRPs

$$v_I = \frac{\bar{z}\bar{v}_0 + zv_0}{\bar{z} + z} + \frac{\sigma_0 - \bar{\sigma}_0}{\bar{z} + z}$$
$$\sigma_I = \frac{\bar{z}^{-1}\bar{\sigma}_0 + z^{-1}\sigma_0}{\bar{z}^{-1} + z^{-1}} + \frac{v_0 - \bar{v}_0}{\bar{z}^{-1} + z^{-1}}$$
$$\rho_I = \rho_0(p_I/p_0)^{1/\gamma}$$

- The traditional FSI coupling is the large impedance (mass) limit  $\bar{z} \gg z$ 
  - velocity from solid  $v_I = \bar{v}_0$
  - stress from fluid  $\sigma_I = \sigma_0 = -p_0 + p_e$
- The traditional scheme is unstable for light solids
- The new scheme is stable for any ratio of masses and impedances
- For proofs see JWB, B. Sjögreen, *A normal mode stability analysis of numerical interface conditions for fluid-structure interaction*, Commun. Comput. Phys., **10** (2011)
- Note: for some difficult problems there are advantages to using the nonlinear FSRP

## We derive a smooth solution to the elastic piston problem for verification

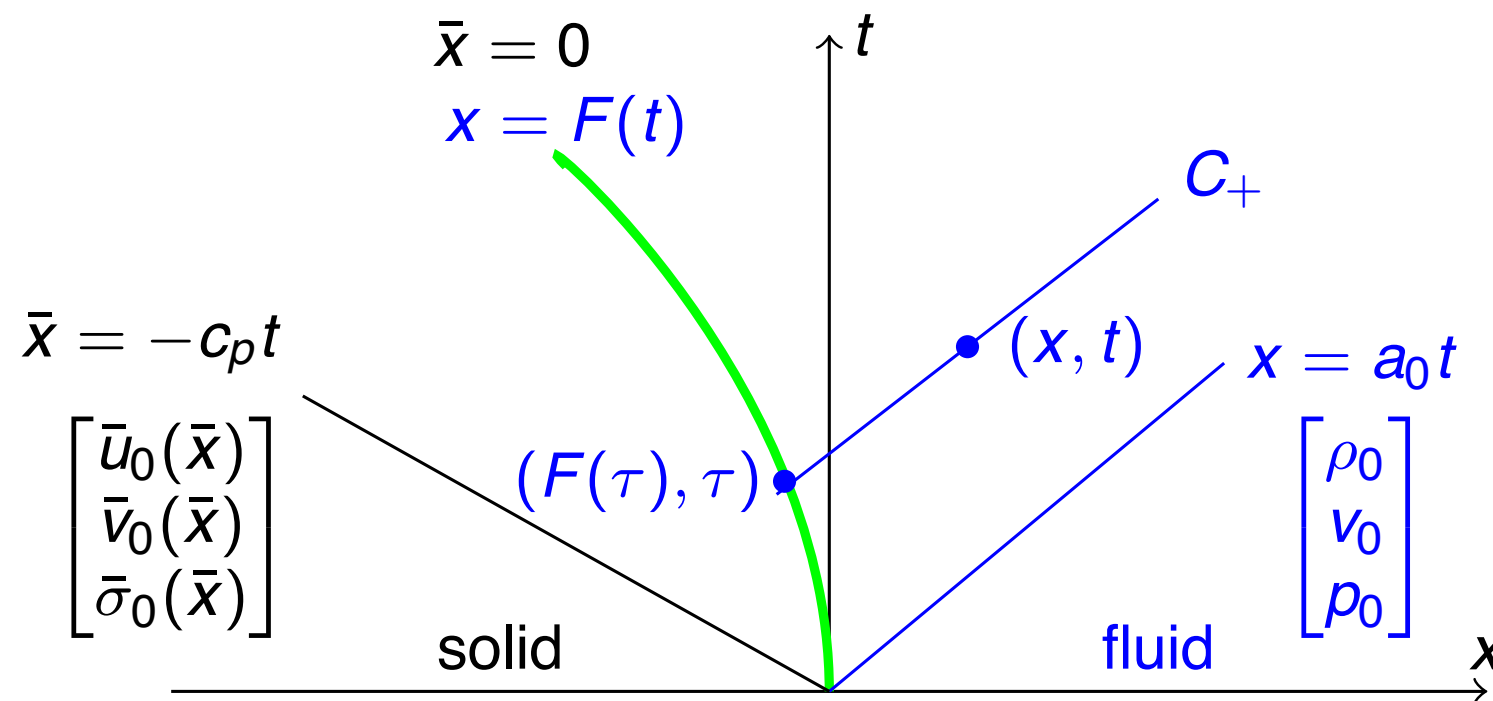


- We pick an interface motion  $F(t)$  and determine initial conditions to produce it
- Choose  $F(t) = -\frac{F_a}{q} t^q$  and a constant initial state in the fluid
- No shocks form in the fluid because  $\dot{F} \leq 0$  and  $\ddot{F} \leq 0$
- Initial conditions for the solid which yield this motion are then determined

$$\bar{u}_0(\bar{x}) = -\frac{p_0}{\bar{\rho}_0 c_p^2} \int_0^{\bar{x}} \left[ 1 + \frac{\gamma - 1}{2a_0} \dot{F}(-s/c_p) \right]^{2\gamma/(\gamma-1)} ds$$

$$\bar{v}_0(\bar{x}) = \dot{F}(-\bar{x}/c_p)$$

## We derive a smooth solution to the elastic piston problem for verification

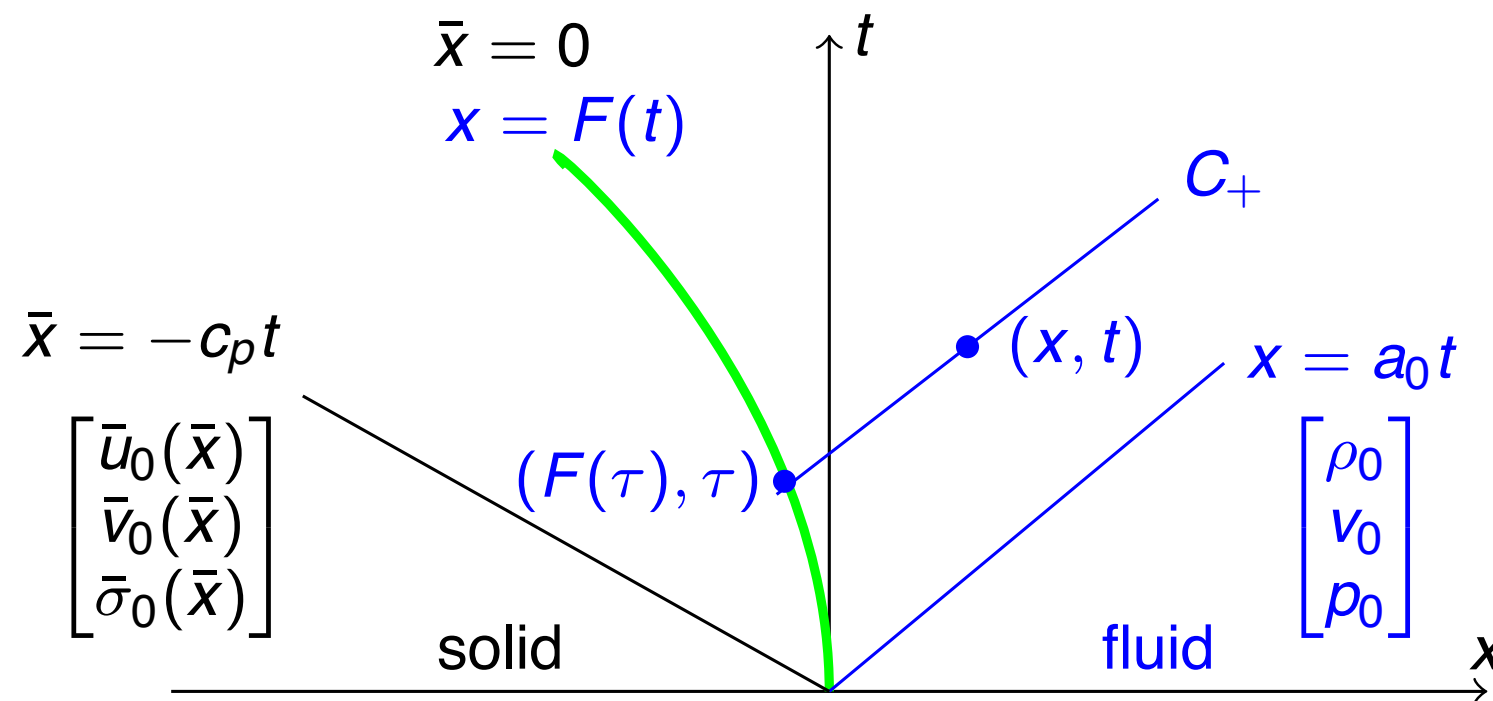


- We pick an interface motion  $F(t)$  and determine initial conditions to produce it
- Choose  $F(t) = -\frac{F_a}{q}t^q$  and a constant initial state in the fluid
- No shocks form in the fluid because  $\dot{F} \leq 0$  and  $\ddot{F} \leq 0$
- Initial conditions for the solid which yield this motion are then determined

$$\bar{u}_0(\bar{x}) = -\frac{p_0}{\bar{\rho}_0 c_p^2} \int_0^{\bar{x}} \left[ 1 + \frac{\gamma - 1}{2a_0} \dot{F}(-s/c_p) \right]^{2\gamma/(\gamma-1)} ds$$

$$\bar{v}_0(\bar{x}) = \dot{F}(-\bar{x}/c_p)$$

## We derive a smooth solution to the elastic piston problem for verification



- We pick an interface motion  $F(t)$  and determine initial conditions to produce it
- Choose  $F(t) = -\frac{F_a}{q} t^q$  and a constant initial state in the fluid
- No shocks form in the fluid because  $\dot{F} \leq 0$  and  $\ddot{F} \leq 0$
- Initial conditions for the solid which yield this motion are then determined

$$\bar{u}_0(\bar{x}) = -\frac{p_0}{\bar{\rho}_0 c_p^2} \int_0^{\bar{x}} \left[ 1 + \frac{\gamma - 1}{2a_0} \dot{F}(-s/c_p) \right]^{2\gamma/(\gamma-1)} ds$$

$$\bar{v}_0(\bar{x}) = \dot{F}(-\bar{x}/c_p)$$

Our DCG-FDI scheme is verified to be second-order accurate in the max norm for very light, and very heavy solid cases

- Choose  $q = 4$  and  $F_a = 1$

very light solid

		Fluid						Solid					
grid	N	$\rho$	r	$v$	r	$p$	r	$\bar{u}$	r	$\bar{v}$	r	$\bar{\sigma}$	r
$G_1$	20	2.7e-03		2.1e-03		1.3e-03		3.9e-04		1.2e-04		1.6e-04	
$G_2$	40	6.1e-04	4.5	5.2e-04	4.1	3.1e-04	4.2	9.7e-05	4.1	3.4e-05	3.6	3.2e-05	5.2
$G_3$	80	1.4e-04	4.2	1.1e-04	4.5	7.9e-05	3.9	2.4e-05	4.1	8.5e-06	4.0	6.9e-06	4.6
$G_4$	160	3.5e-05	4.2	3.0e-05	3.9	2.0e-05	4.0	5.9e-06	4.0	2.1e-06	4.0	1.6e-06	4.3
rate		2.10		2.06		2.01		2.02		1.95		2.23	

$$\bar{\rho} = 1 \times 10^{-5}, \bar{z}/z = 1.7 \times 10^{-4}$$

very heavy solid

		Fluid						Solid					
grid	N	$\rho$	r	$v$	r	$p$	r	$\bar{u}$	r	$\bar{v}$	r	$\bar{\sigma}$	r
$G_1$	20	1.6e-03		1.3e-03		1.1e-03		2.4e-04		1.7e-05		1.6e-05	
$G_2$	40	3.2e-04	4.9	2.8e-04	4.8	2.2e-04	5.2	5.9e-05	4.0	4.0e-06	4.3	3.7e-06	4.3
$G_3$	80	6.7e-05	4.8	5.0e-05	5.6	4.6e-05	4.7	1.4e-05	4.1	9.4e-07	4.2	9.0e-07	4.1
$G_4$	160	1.7e-05	4.0	1.2e-05	4.1	1.1e-05	4.0	3.6e-06	4.0	2.3e-07	4.1	2.3e-07	3.9
rate		2.19		2.28		2.22		2.02		2.07		2.03	

$$\bar{\rho} = 1 \times 10^5, \bar{z}/z = 1.7 \times 10^6$$

Our DCG-FDI scheme is verified to be second-order accurate in the max norm for very light, and very heavy solid cases

- Choose  $q = 4$  and  $F_a = 1$

**very light solid**

		Fluid						Solid					
grid	N	$\rho$	r	$v$	r	$p$	r	$\bar{u}$	r	$\bar{v}$	r	$\bar{\sigma}$	r
$G_1$	20	2.7e-03		2.1e-03		1.3e-03		3.9e-04		1.2e-04		1.6e-04	
$G_2$	40	6.1e-04	4.5	5.2e-04	4.1	3.1e-04	4.2	9.7e-05	4.1	3.4e-05	3.6	3.2e-05	5.2
$G_3$	80	1.4e-04	4.2	1.1e-04	4.5	7.9e-05	3.9	2.4e-05	4.1	8.5e-06	4.0	6.9e-06	4.6
$G_4$	160	3.5e-05	4.2	3.0e-05	3.9	2.0e-05	4.0	5.9e-06	4.0	2.1e-06	4.0	1.6e-06	4.3
rate		2.10		2.06		2.01		2.02		1.95		2.23	

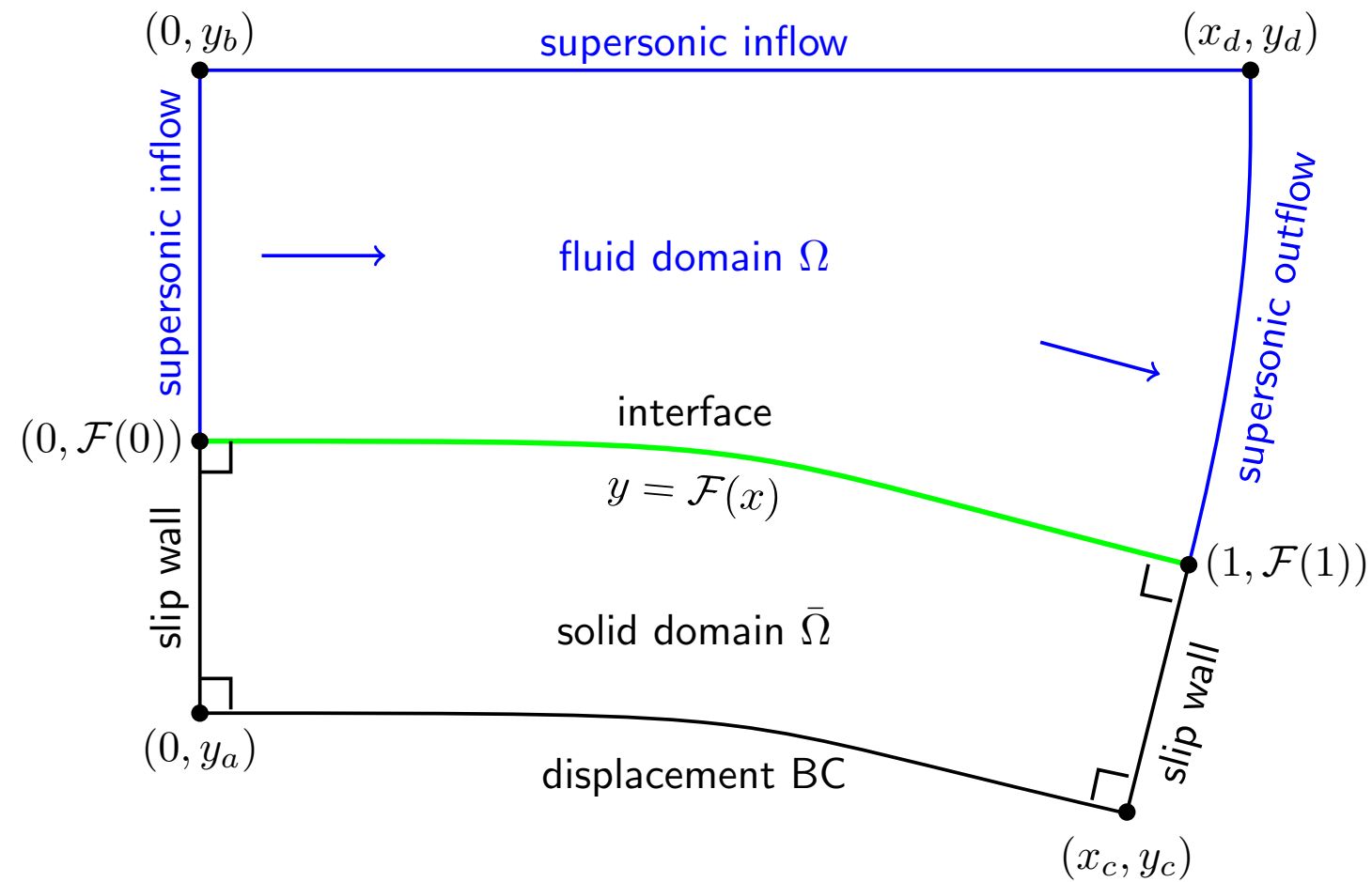
$$\bar{\rho} = 1 \times 10^{-5}, \bar{z}/z = 1.7 \times 10^{-4}$$

**very heavy solid**

		Fluid						Solid					
grid	N	$\rho$	r	$v$	r	$p$	r	$\bar{u}$	r	$\bar{v}$	r	$\bar{\sigma}$	r
$G_1$	20	1.6e-03		1.3e-03		1.1e-03		2.4e-04		1.7e-05		1.6e-05	
$G_2$	40	3.2e-04	4.9	2.8e-04	4.8	2.2e-04	5.2	5.9e-05	4.0	4.0e-06	4.3	3.7e-06	4.3
$G_3$	80	6.7e-05	4.8	5.0e-05	5.6	4.6e-05	4.7	1.4e-05	4.1	9.4e-07	4.2	9.0e-07	4.1
$G_4$	160	1.7e-05	4.0	1.2e-05	4.1	1.1e-05	4.0	3.6e-06	4.0	2.3e-07	4.1	2.3e-07	3.9
rate		2.19		2.28		2.22		2.02		2.07		2.03	

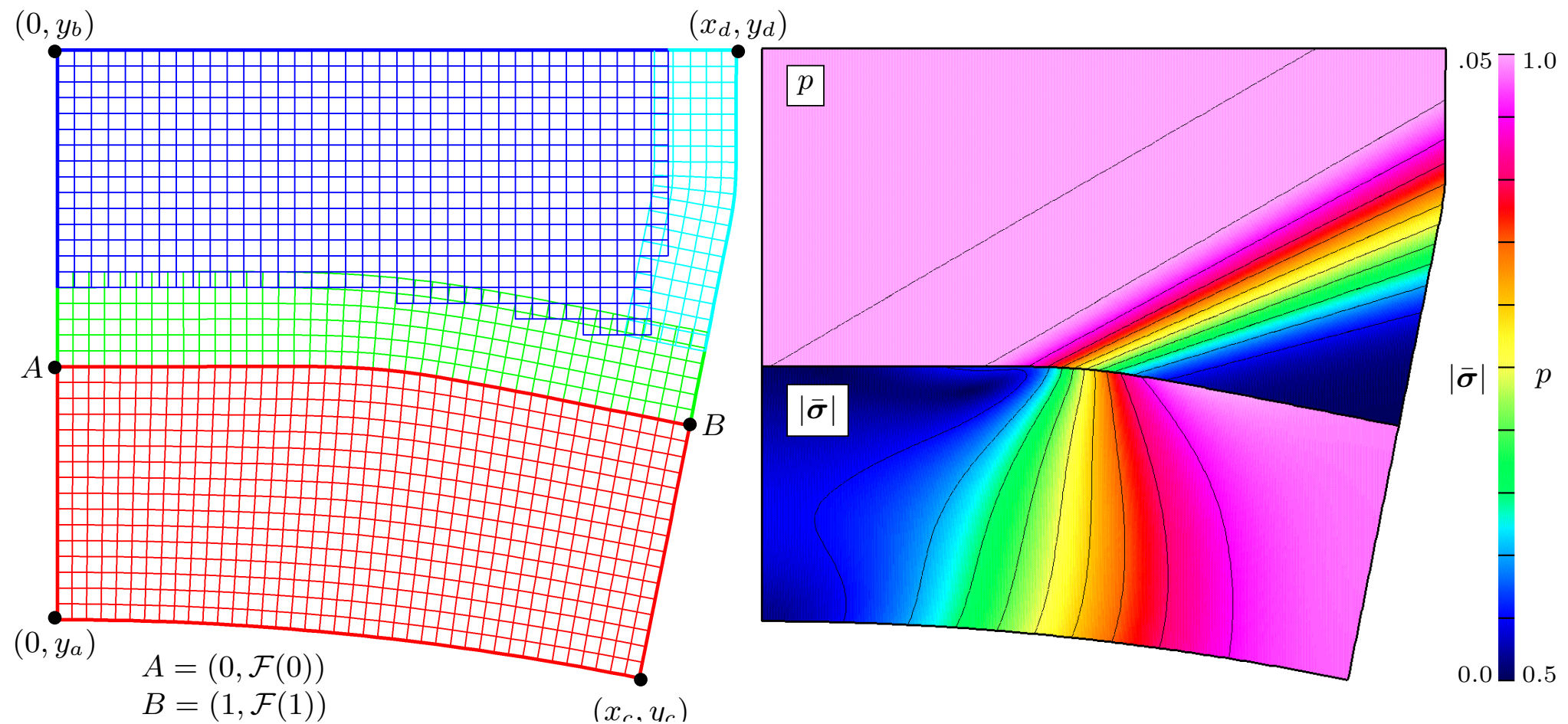
$$\bar{\rho} = 1 \times 10^5, \bar{z}/z = 1.7 \times 10^6$$

## The deforming diffuser solution can be used to investigate convergence in 2D



- A coupled semi-analytic smooth solution is determined:
  - Fluid: Prandtl-Meyer analytic solution as a function of  $F(x)$
  - Solid: steady elasticity equations are solved on a very fine grid
  - The coupled exact solution and  $F(x)$  are determined by iteration

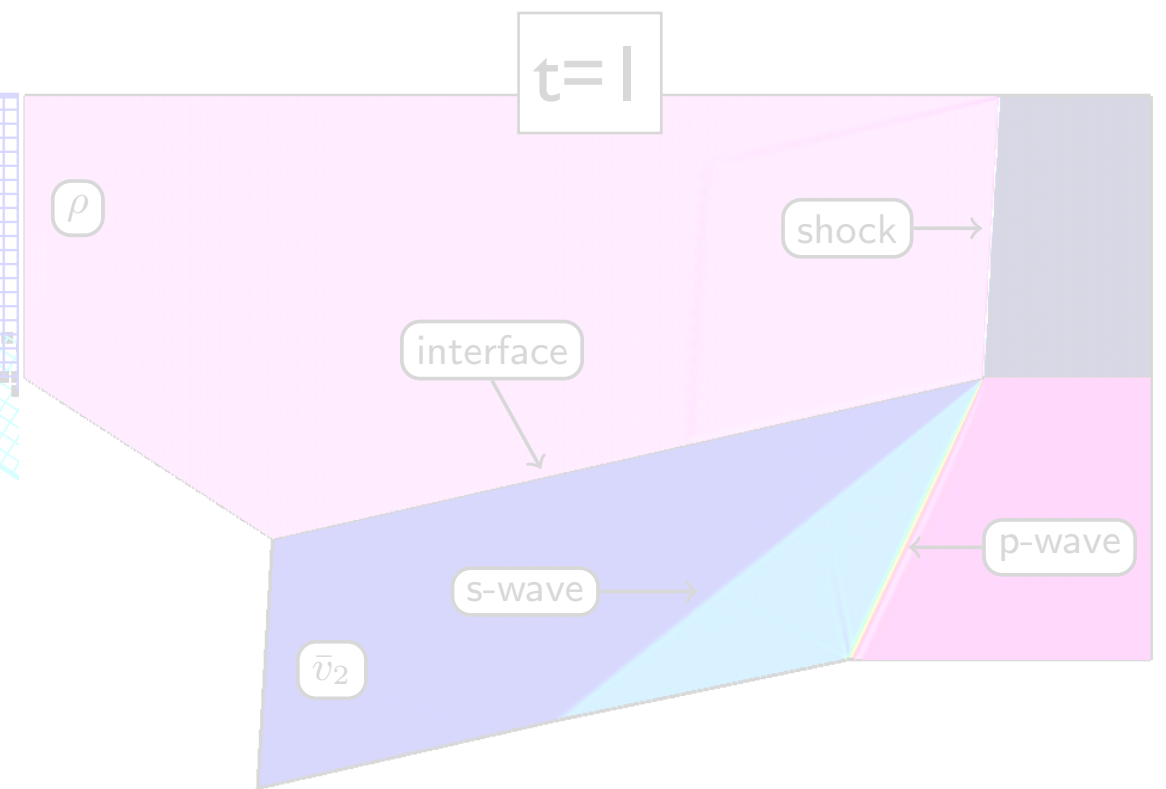
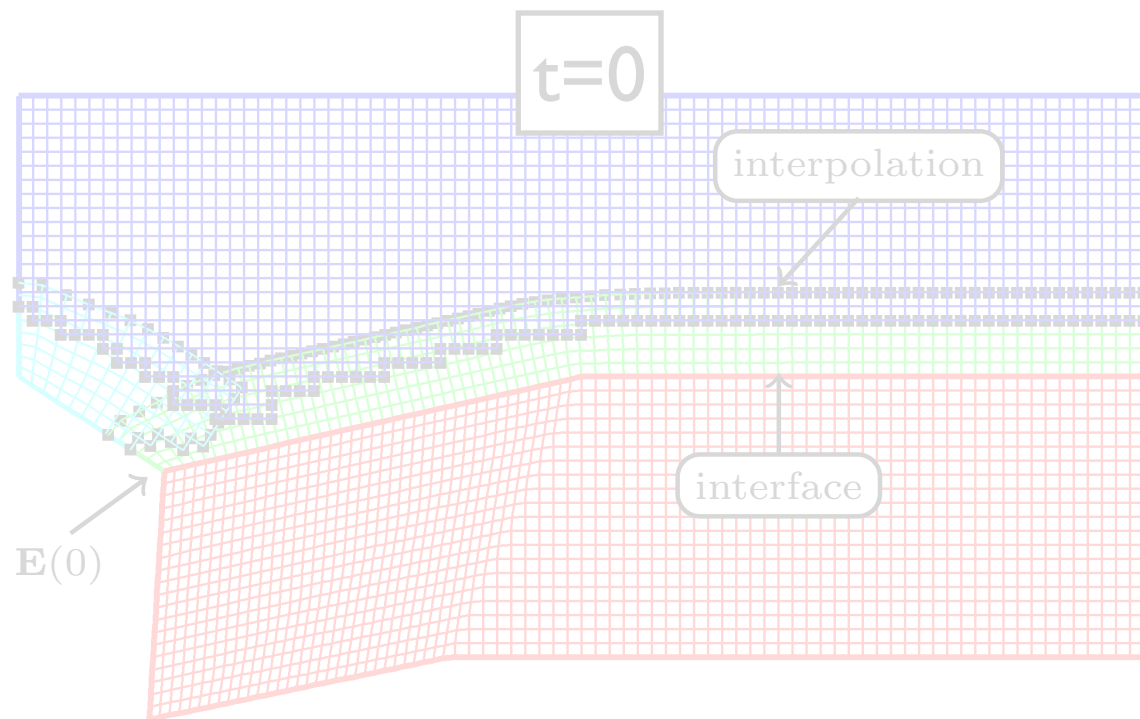
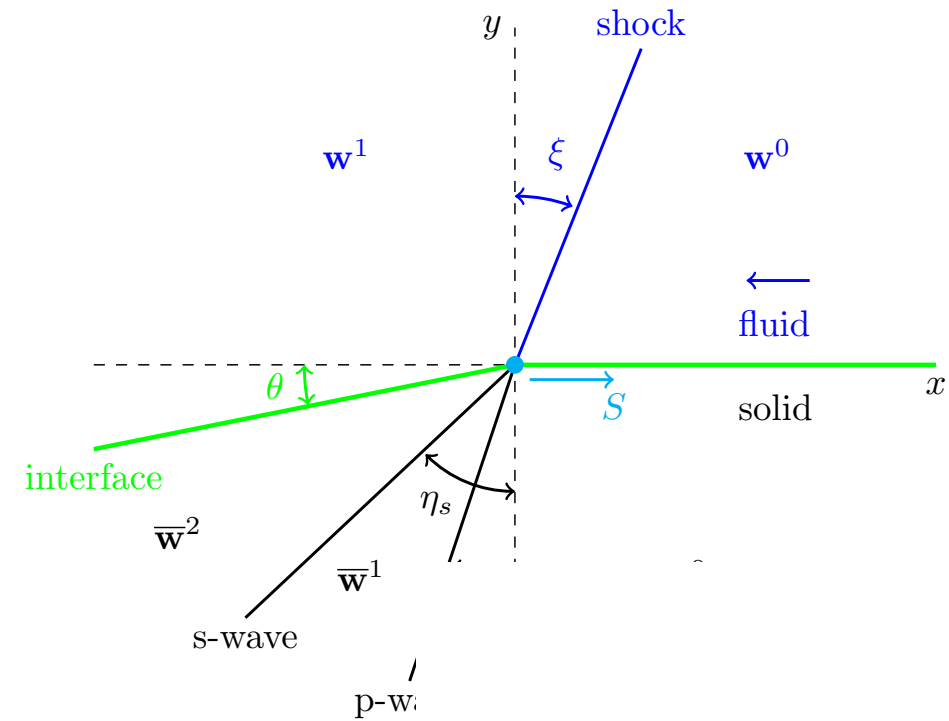
# The deforming diffuser solution can be used to investigate convergence in 2D



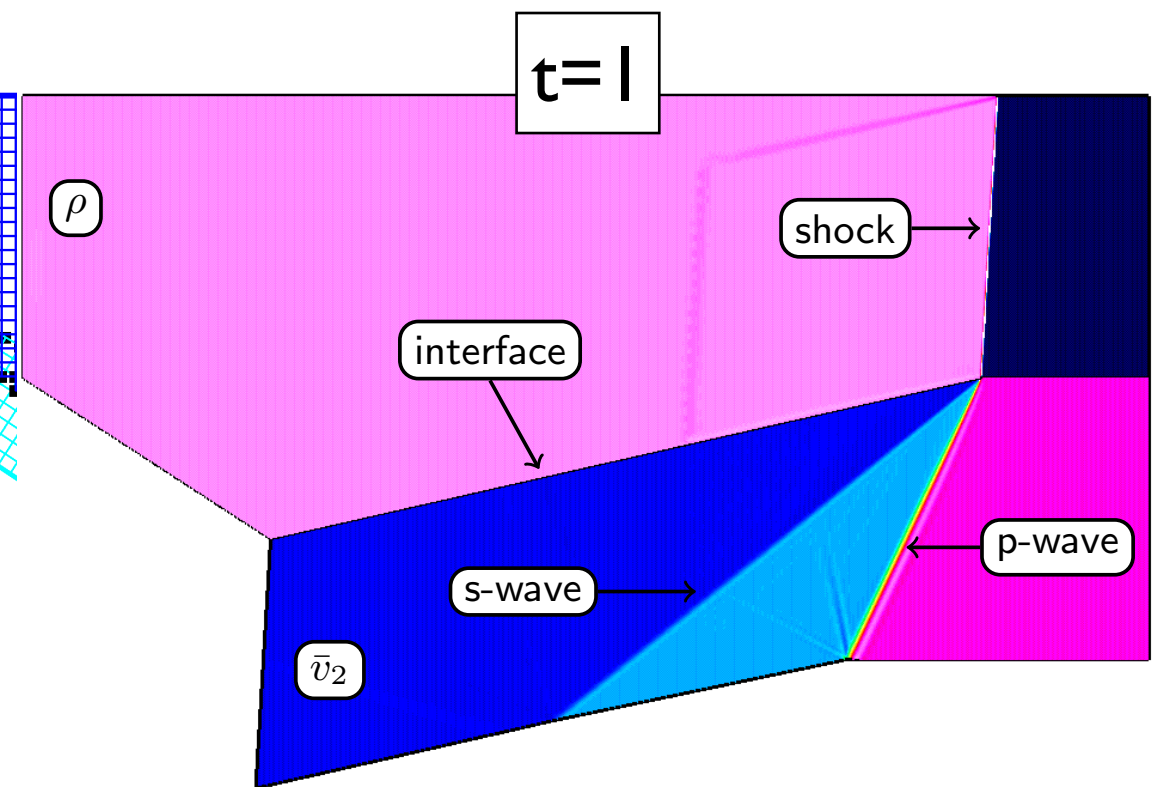
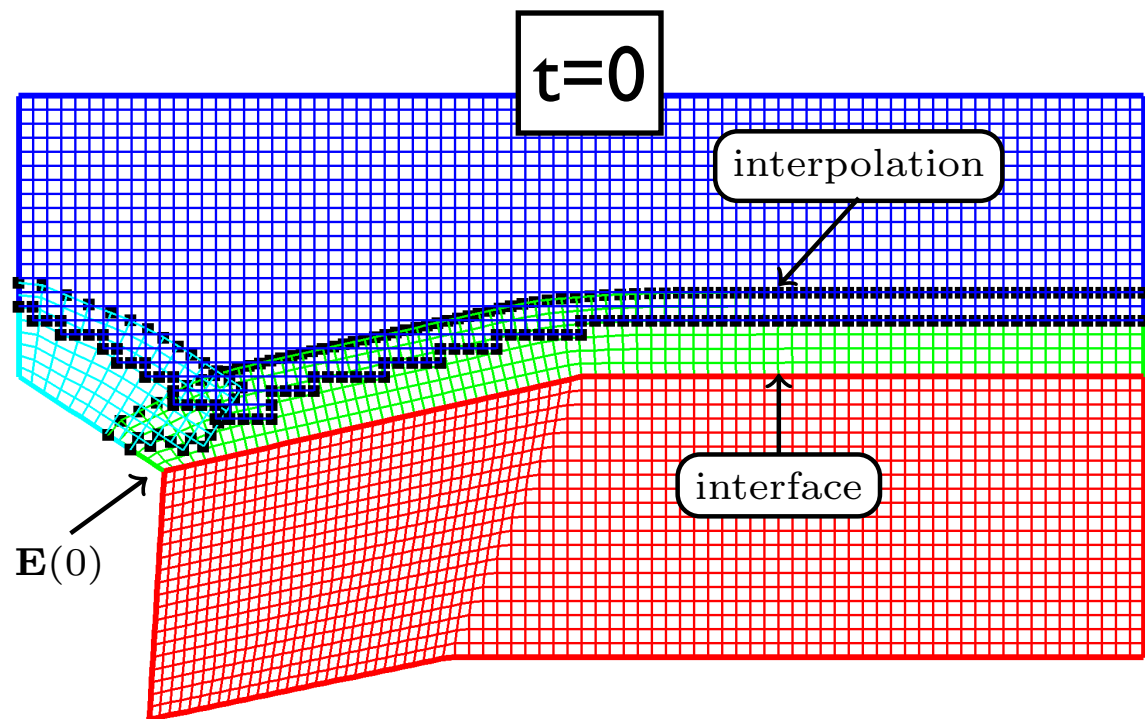
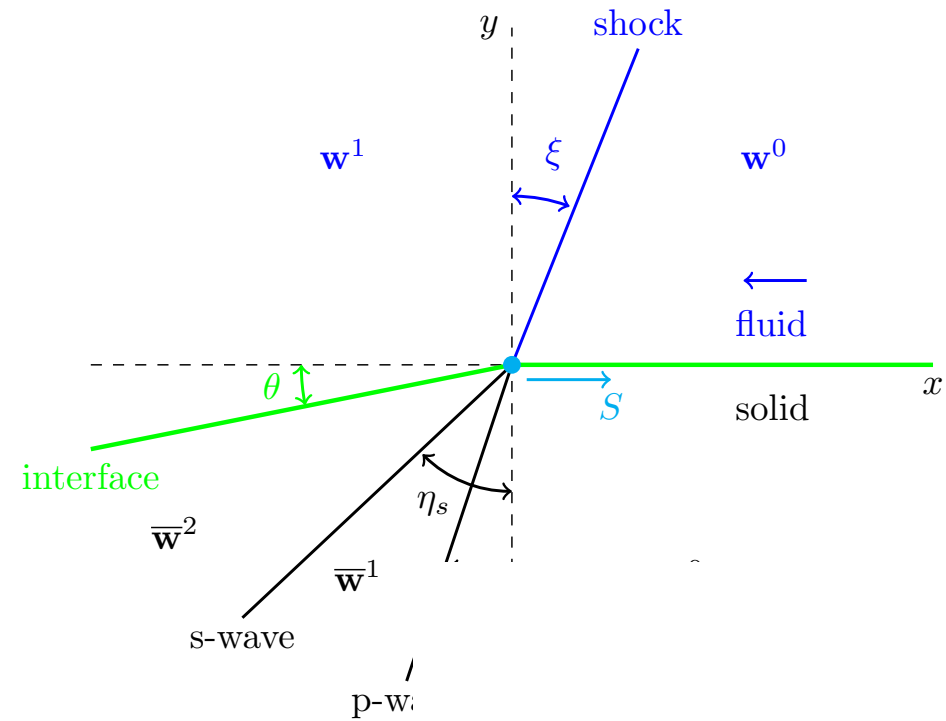
Grid	Solid						Fluid					
	$\mathcal{E}_{\bar{u}}^{(\infty)}$	r	$\mathcal{E}_{\bar{v}}^{(\infty)}$	r	$\mathcal{E}_{\bar{\sigma}}^{(\infty)}$	r	$\mathcal{E}_{\rho}^{(\infty)}$	r	$\mathcal{E}_{\mathbf{v}}^{(\infty)}$	r	$\mathcal{E}_T^{(\infty)}$	r
$\mathcal{G}_{dd}^{(2)}$	1.6e-4		2.8e-4		2.9e-2		3.4e-2		2.1e-2		7.0e-3	
$\mathcal{G}_{dd}^{(4)}$	3.3e-5	4.8	1.1e-4	2.6	8.9e-3	3.3	8.6e-3	3.9	6.3e-3	3.4	1.9e-3	3.8
$\mathcal{G}_{dd}^{(8)}$	5.6e-6	5.9	2.8e-5	3.9	1.8e-3	5.0	2.2e-3	3.8	2.1e-3	3.0	5.9e-4	3.2
$\mathcal{G}_{dd}^{(16)}$	9.4e-7	5.9	6.8e-6	4.1	3.5e-4	5.0	5.8e-4	3.8	4.7e-4	4.4	1.3e-4	4.4
rate	2.48		1.81		2.14		1.95		1.81		1.88	

- Max norm convergence verifies second-order accuracy

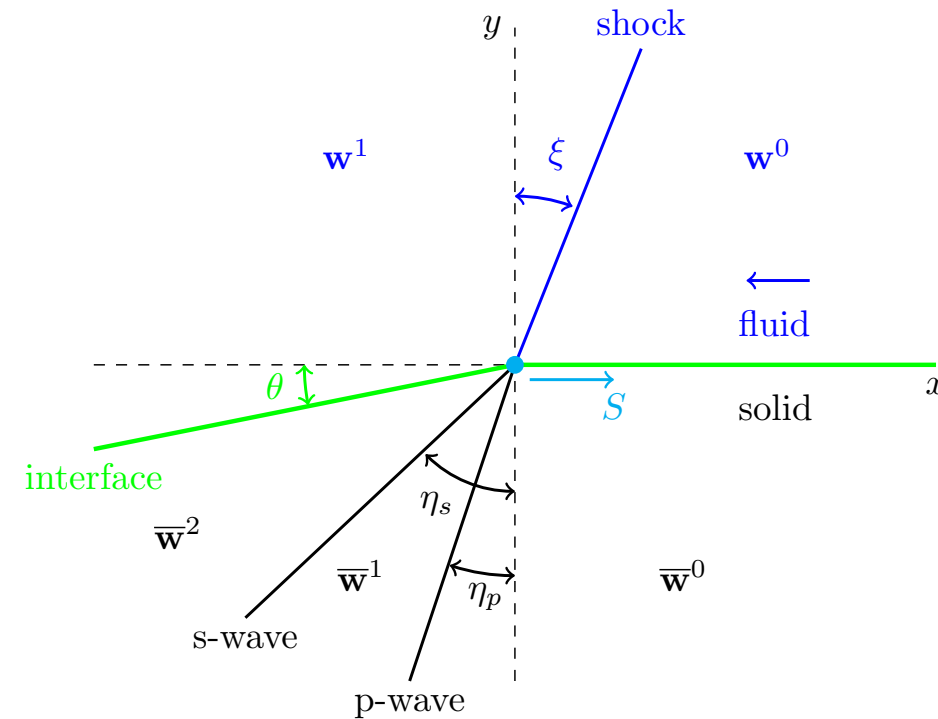
# The superseismic shock problem is used to demonstrate convergence for problems with discontinuities



# The superseismic shock problem is used to demonstrate convergence for problems with discontinuities



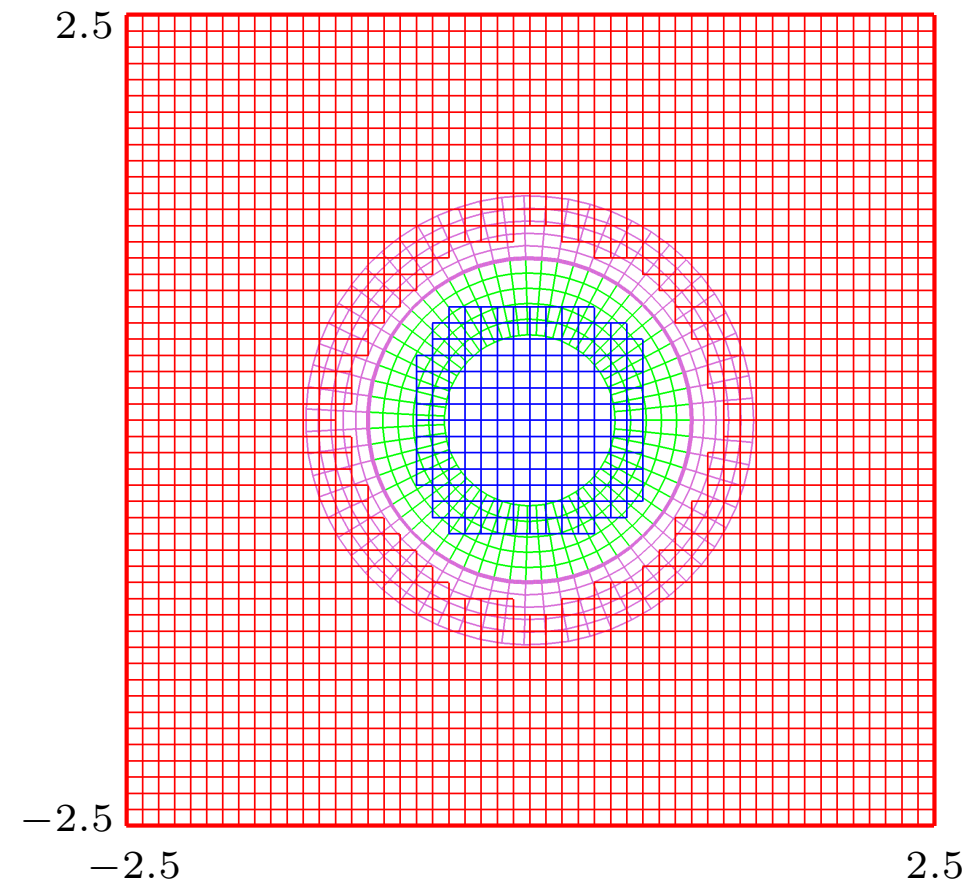
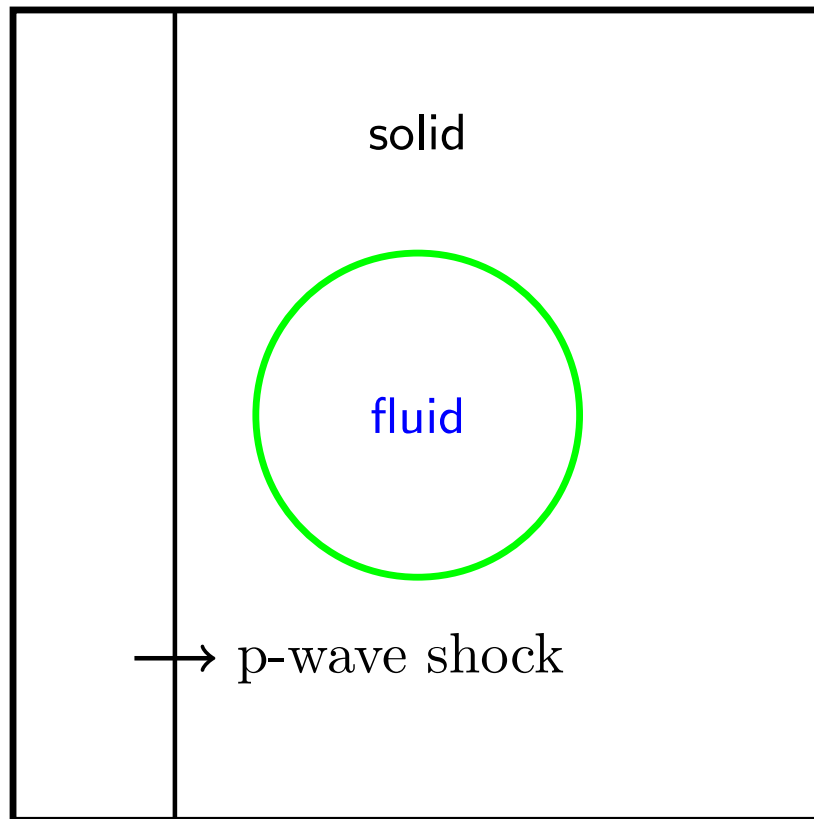
# The superseismic shock problem is used to demonstrate convergence for problems with discontinuities



- L-1 norm convergence results demonstrate expected behavior

Grid	Solid						Fluid					
	$\mathcal{E}_{\bar{\mathbf{u}}}^{(1)}$	r	$\mathcal{E}_{\bar{\mathbf{v}}}^{(1)}$	r	$\mathcal{E}_{\bar{\sigma}}^{(1)}$	r	$\mathcal{E}_{\rho}^{(1)}$	r	$\mathcal{E}_{\mathbf{v}}^{(1)}$	r	$\mathcal{E}_T^{(1)}$	r
$\mathcal{G}_{SS}^{(4)}$	8.9e-4		6.4e-3		1.8e-2		5.9e-3		3.8e-2		1.2e-2	
$\mathcal{G}_{SS}^{(8)}$	3.2e-4	2.8	3.9e-3	1.6	1.1e-2	1.6	2.9e-3	2.0	1.7e-2	2.2	6.7e-3	1.8
$\mathcal{G}_{SS}^{(16)}$	1.4e-4	2.4	2.4e-3	1.7	6.7e-3	1.7	1.6e-3	1.9	8.6e-3	2.0	3.7e-3	1.8
$\mathcal{G}_{SS}^{(32)}$	6.7e-5	2.0	1.4e-3	1.6	4.1e-3	1.6	8.2e-4	1.9	4.3e-3	2.0	1.9e-3	1.9
rate	1.24		0.72		0.72		0.94		1.03		0.88	

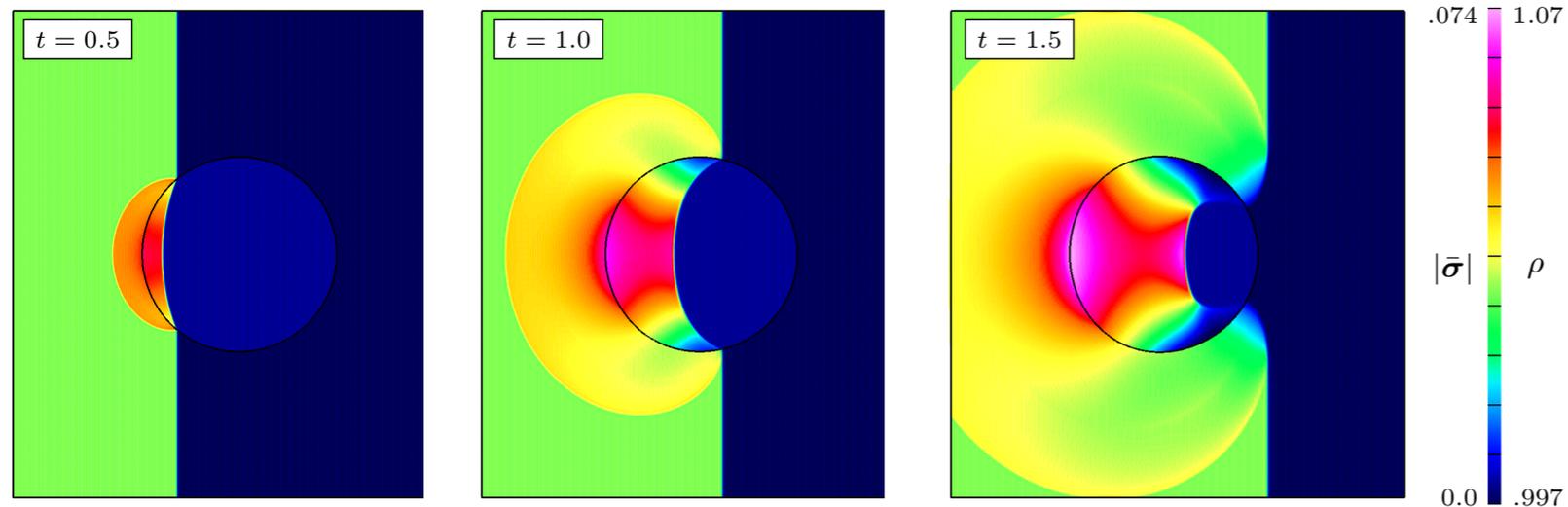
# Self-convergence is measured for a difficult problem of a fluid cylinder impacted by a solid compression wave



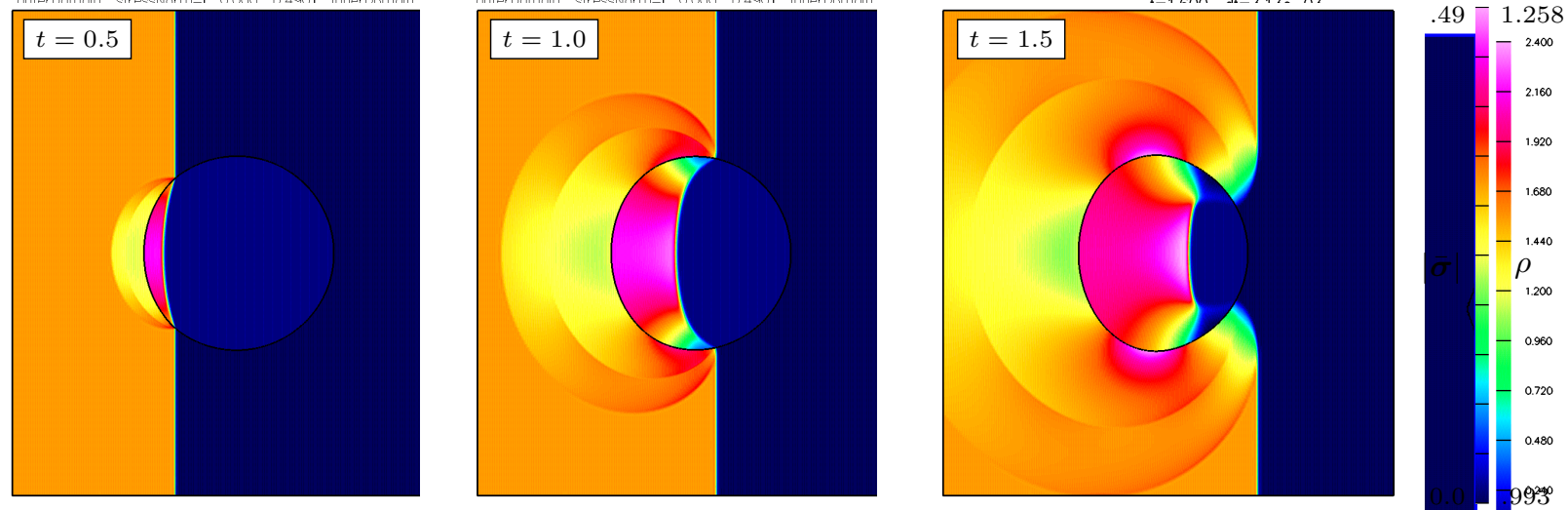
- L-1 norm convergence results demonstrate expected behavior

Grid	Solid						Fluid					
	$\mathcal{E}_{\bar{\mathbf{u}}}^{(1)}$	r	$\mathcal{E}_{\bar{\mathbf{v}}}^{(1)}$	r	$\mathcal{E}_{\bar{\sigma}}^{(1)}$	r	$\mathcal{E}_{\rho}^{(1)}$	r	$\mathcal{E}_{\mathbf{v}}^{(1)}$	r	$\mathcal{E}_T^{(1)}$	r
$\mathcal{G}_{dc}^{(4)}$	1.7e-4		1.1e-3		1.3e-3		4.1e-3		2.3e-3		4.2e-3	
$\mathcal{G}_{dc}^{(8)}$	7.9e-5	2.1	6.9e-4	1.6	7.9e-4	1.6	2.2e-3	1.8	1.3e-3	1.8	2.3e-3	1.8
$\mathcal{G}_{dc}^{(64)}$	8.3e-6	9.5	1.5e-4	4.5	1.8e-4	4.3	3.6e-4	6.3	2.1e-4	6.1	3.7e-4	6.2
rate	1.08		0.72		0.71		0.88		0.87		0.88	

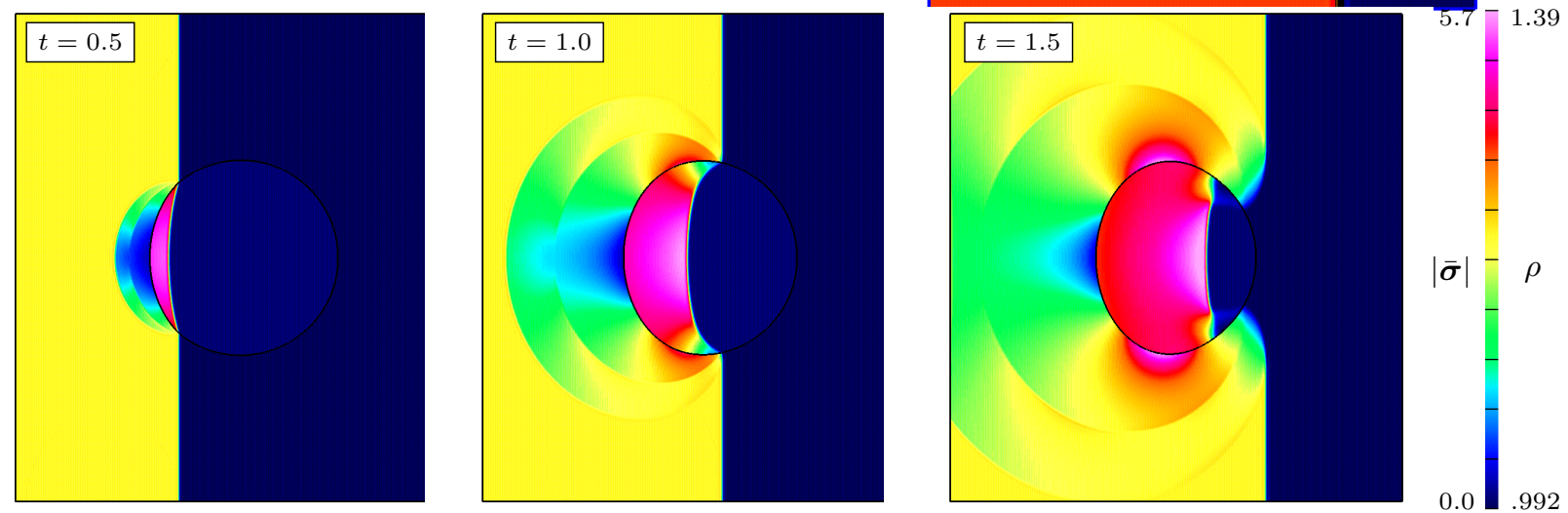
# Stability for a variety of fluid/solid ratios is demonstrated



light solid  
 $\bar{\rho} = 0.1$

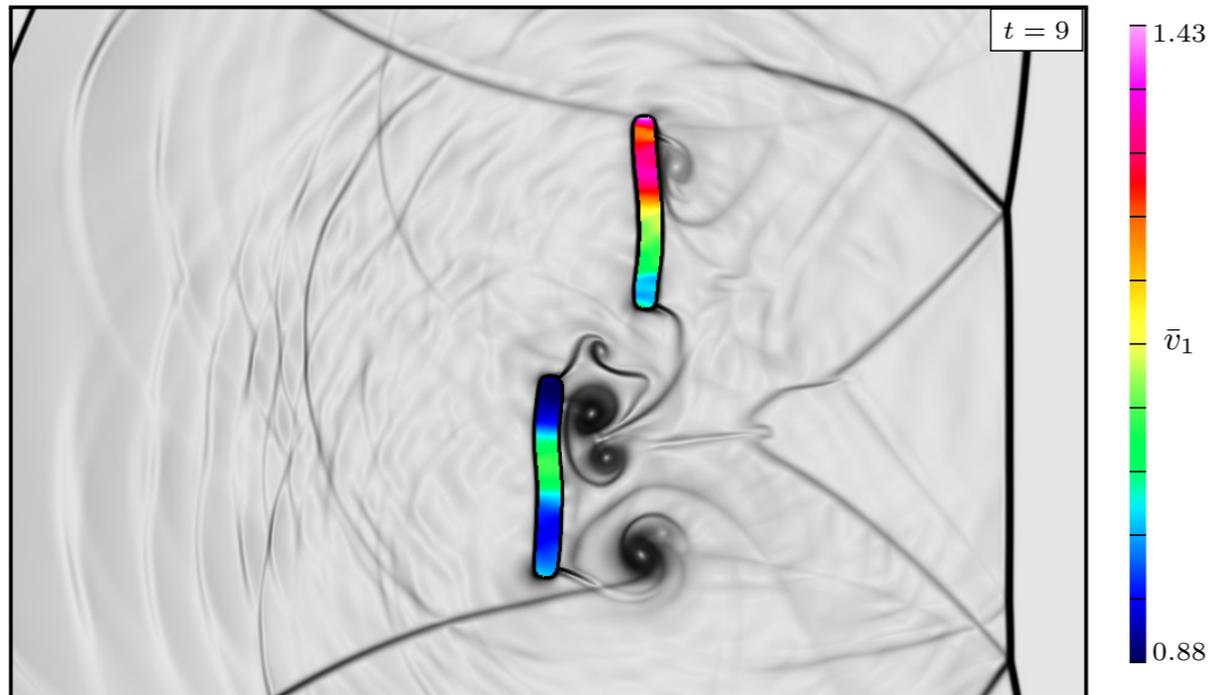


medium solid  
 $\bar{\rho} = 1.0$

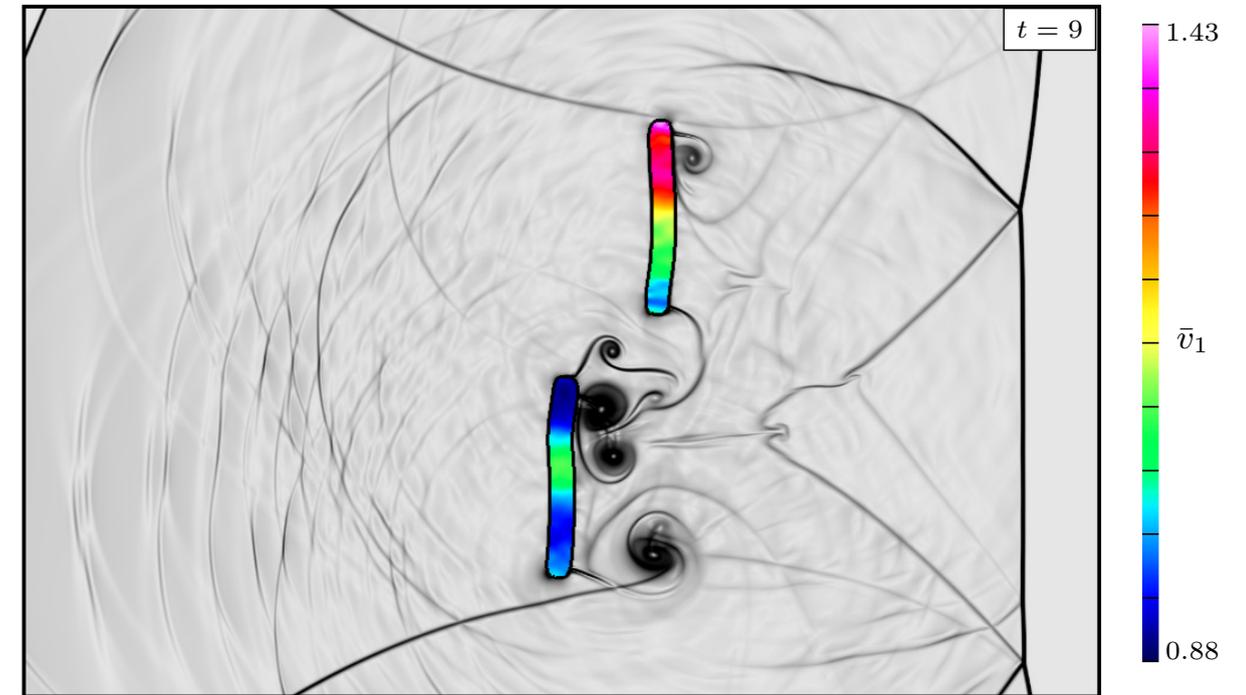


heavy solid  
 $\bar{\rho} = 10.0$

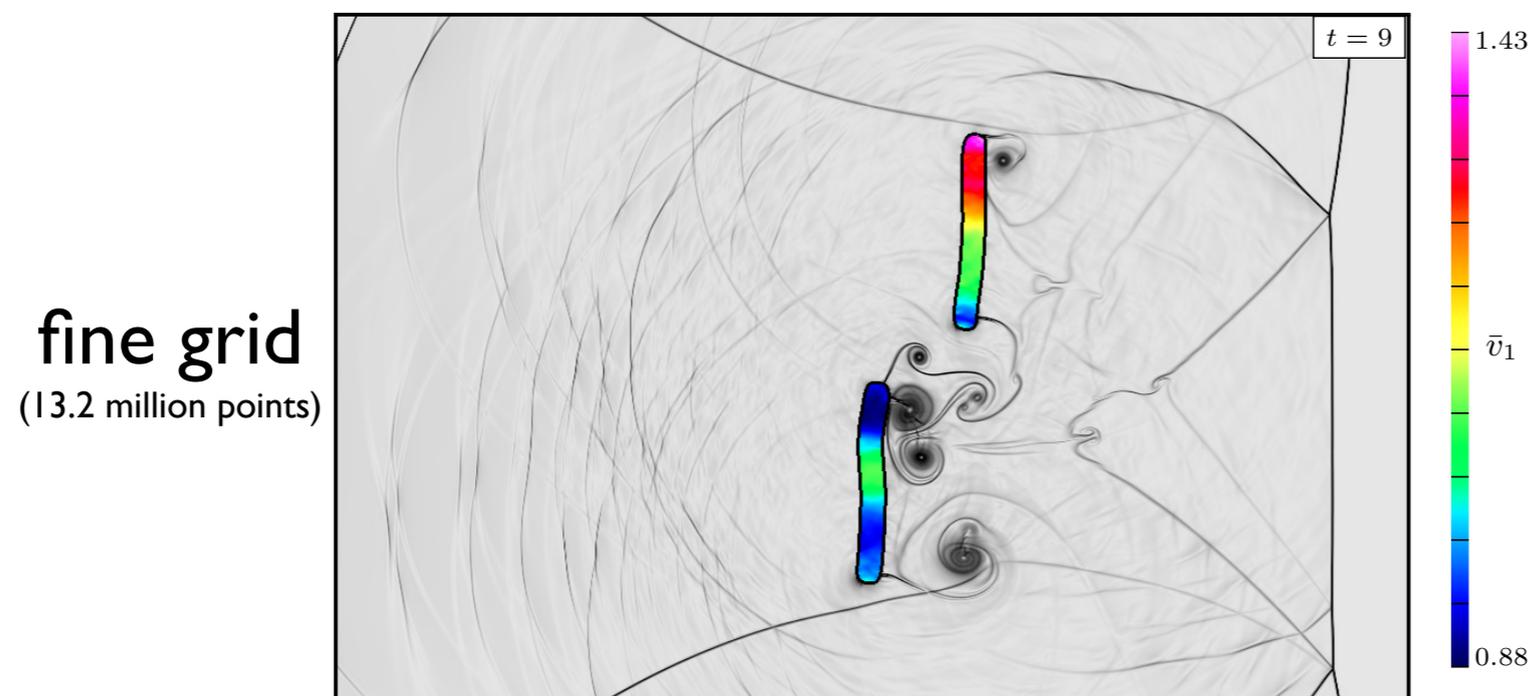
As a final illustration, we return to the deforming sticks example to show the efficacy of the DCG approach for problems with large displacements



**coarse grid**  
(.8 million points)



**medium grid**  
(3.3 million points)



**fine grid**  
(13.2 million points)

## Summary

- The deforming composite grid approach was developed for coupling high-speed compressible fluids to elastic solids
- Stability was achieved for light and heavy solids using an interface projection technique which is motivated by the solution to a fluid-solid Riemann problem
- Second-order convergence in the max-norm was verified for smooth flows in both one and two space dimensions
- Convergence of the L-1 norm for more difficult problems involving shocks was shown to agree with predicted theory

## Future work

- Continue development of DCGs to include AMR
- Move to more general solid models (nonlinear solids, beams, plates, etc ...)
- Extend analysis and methodology to incompressible fluids
- Extend analysis and methodology to light rigid bodies
- Move to three dimensions